analytical chemistry

pubs.acs.org/ac Article

Strategy for Identifying a Robust Metabolomic Signature Reveals the Altered Lipid Metabolism in Pituitary Adenoma

Jing Tang,[#] Minjie Mou,[#] Xin Zheng,[#] Jin Yan, Ziqi Pan, Jinsong Zhang, Bo Li, Qingxia Yang, Yunxia Wang, Ying Zhang, Jianqing Gao, Song Li,* Hui Yang,* and Feng Zhu*

Cite This: https://doi.org/10.1021/acs.analchem.3c03796 Read Online

ACCESS | Metrics & More | Article Recommendations | Supporting Information

ABSTRACT: Despite the well-established connection between systematic metabolic abnormalities and the pathophysiology of pituitary adenoma (PA), current metabolomic studies have reported an extremely limited number of metabolites associated with PA. Moreover, there was very little consistency in the identified metabolite signatures, resulting in a lack of robust metabolic biomarkers for the diagnosis and treatment of PA. Herein, we performed a global untargeted plasma metabolomic profiling on PA and identified a highly robust metabolomic signature based on a strategy. Specifically, this strategy is unique in (1) integrating repeated random sampling and a consensus evaluation-based feature selection algorithm and (2) evaluating the consistency of metabolomic signatures among different sample groups. This strategy demonstrated superior robustness and stronger discriminative ability compared with that of other feature selection methods including Student's *t*-test, partial least-squares-discriminant analysis, support vector machine recursive feature elimination, and random forest recursive feature elimination. More importantly, a highly robust metabolomic signature comprising 45 PA-specific differential metabolites was identified. Moreover, metabolite set enrichment analysis of these potential metabolic biomarkers revealed altered lipid metabolism in PA. In conclusion, our findings contribute to a better understanding of the metabolic changes in PA and may have implications for the development of diagnostic and therapeutic approaches targeting lipid metabolism in PA. We believe that the proposed strategy serves as a valuable tool for screening robust, discriminating metabolic features in the field of metabolomics.

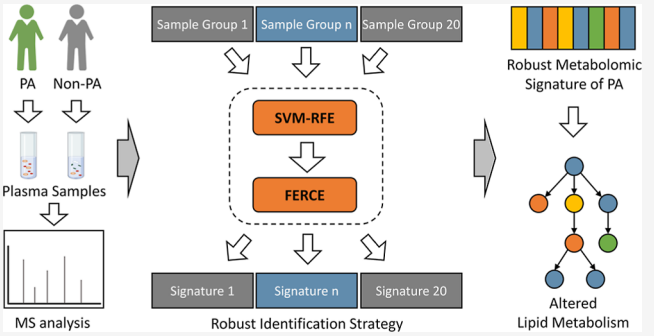

INTRODUCTION

Pituitary adenoma (PA) is one of the most common intracranial and neuroendocrine neoplasms with high prevalence,[1−4] which accounts for a large proportion of intracranial tumors.[1,5,6] Due to its aggressive infiltration into the surrounding brain tissue and its severe complications (such as Cushing's disease, hyperprolactinemia, and acromegaly),[7−9] it is essential to unveil the molecular mechanisms underlying the development of PA,[10] which can effectively facilitate the discovery of novel therapeutics.[10] Systematic metabolic abnormalities have been reported to closely correlate with the development, progression, and prognosis of PA,[11,12] which has made the identification of differential metabolites between PA and healthy individuals a popular field.[11]

Currently, due to the inaccessibility of the pituitary gland for biopsy and the lack of relevant cell lines and animal models, the understanding of metabolic abnormalities during the pathogenesis of PA remains an extremely challenging problem.[11,13,14] Several publications have in-depth studied the systemic metabolic abnormalities in the pathogenesis of PA using high-throughput metabolomics techniques.[10,14−16] Specifically, Oklu et al. investigated the cellular secretions of ACTH using plasma derived from bilateral inferior petrosal sinus sampling (BIPSS) blood and found that amino acid metabolism appeared to be primarily altered in PA.[14] Ijare et al. used NMR spectrometry to assess the metabolomic profile of PA and identified that the aspartate and glutamate metabolism was affected in PA.[17] These studies provided preliminary insights into the pathogenesis of PA.

However, among these previous publications, the number of differential metabolites associated with PA was extremely limited, which made it hard to comprehensively study systemic metabolic abnormalities.[14] In addition, the most commonly used methods for screening differential metabolites are partial least-squares-discriminant analysis (PLS-DA), Student's *t*-test, and linear discriminant analysis (LDA).[18,19] However, these statistical methods may have limitations when applied to the

Received: August 24, 2023
Revised: February 5, 2024
Accepted: February 5, 2024

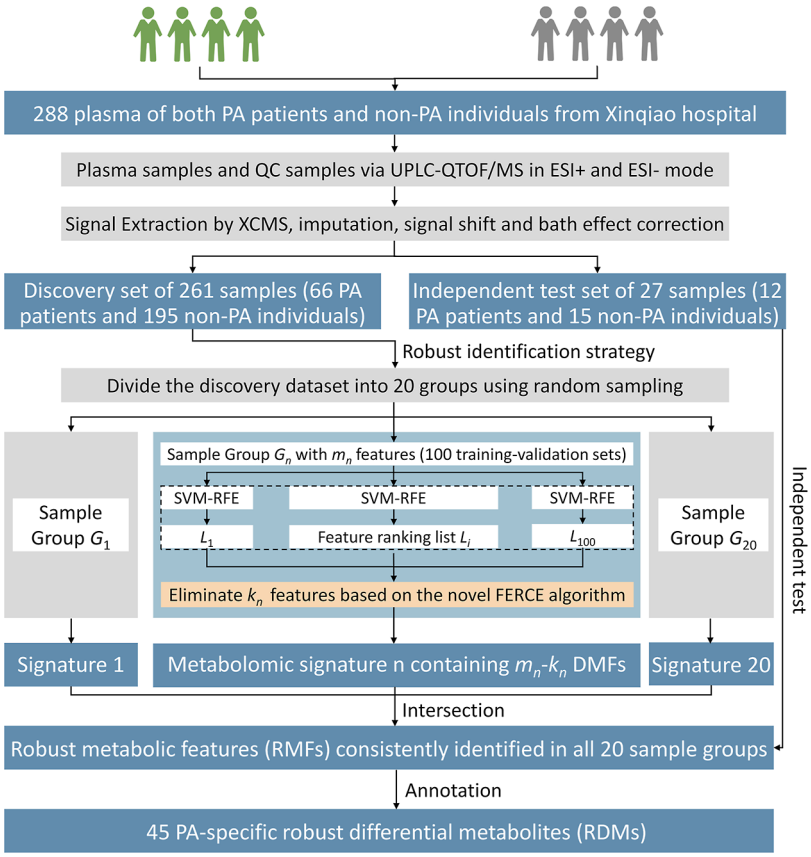

Figure 1. Workflow of the newly constructed robust identification strategy for identifying PA-specific RDMs.

current metabolomic data set.[20] Nonlinear associations were reported among metabolites.[21] Support vector machine-recursive feature elimination (SVM-RFE) has been introduced as a valuable approach for biomarker identification in metabolomic data, specifically designed to tackle issues such as noisy training examples, a limited number of biological replicates,[22] and nonlinearity among metabolites.[21] Moreover, increasing evidence has demonstrated that there is very little consistency in the identified biomarkers among published metabolomic studies.[23−27] This inconsistency among metabolomic signatures from different studies was attributed to several factors,[25] including (i) the inconsistency of samples,[28,29] (ii) the differences of analytical platform,[23] (iii) the insufficiency of sample sizes,[30] and (iv) the subtle variation of the statistical methods employed to identify differential features.[25,31] Therefore, it is essential to develop a novel strategy to discover the highly robust metabolomic signatures of PA and to facilitate the understanding of molecular mechanisms underlying PA pathogenesis based on the robust metabolomic signatures.[24,25,32]

Herein, global plasma metabolomic profiling of PA was performed, and a novel robust identification strategy for identifying the robust metabolomic signature was developed. Specifically, this novel strategy integrates repeated random sampling and a consensus evaluation-based feature selection algorithm and can evaluate the consistency of metabolomic signatures among different sample groups. A systematic assessment from multiple perspectives was conducted to demonstrate the performance of the proposed strategy. The evaluation of spike-in metabolomics data revealed that the proposed algorithm successfully identified a significant number of true positive metabolic features. In comparison with other feature selection methods, the proposed strategy exhibited superior robustness in the selection of metabolite features and demonstrated enhanced predictive ability on the independent test data. Based on this novel strategy, 45 highly robust differential metabolites (RDMs) distinguishing PA from non-PA samples were identified, and the significant plasma metabolic alteration between PA and non-PA patients was clarified. Among all of the identified metabolites, most were reported to be associated with PA for the first time. Moreover, the results of metabolite set enrichment analysis (MSEA) revealed that dysregulation of lipid metabolism was a key factor in the pathogenesis of PA. In conclusion, our study represents the first comprehensive untargeted metabolomic analysis of PA, providing novel insights into robust metabolic biomarkers for PA diagnosis and treatment. The findings highlight the crucial role of lipid metabolism in PA pathogenesis. Furthermore, we assert that the proposed strategy serves as a valuable tool for screening robust, discriminating metabolic features in the metabolomics field.

MATERIALS AND METHODS

Human Subjects. This study enrolled 113 patients with brain tumors with informed consent, and the study protocol was approved by Xinqiao Hospitals, Army Medical University of China. The diagnoses were confirmed via histopathological analyses of surgical specimens obtained from the patients. These diagnosed brain tumors were composed of PAs (n = 78), craniopharyngioma (n = 10), Rathke cleft cysts (n = 11), meningiomas (n = 5), gliomas (n = 2), arachnoid cysts (n = 3), and intracranial germinoma (n = 4) according to the 2004

https://doi.org/10.1021/acs.analchem.3c03796
Anal. Chem. XXXX, XXX, XXX−XXX

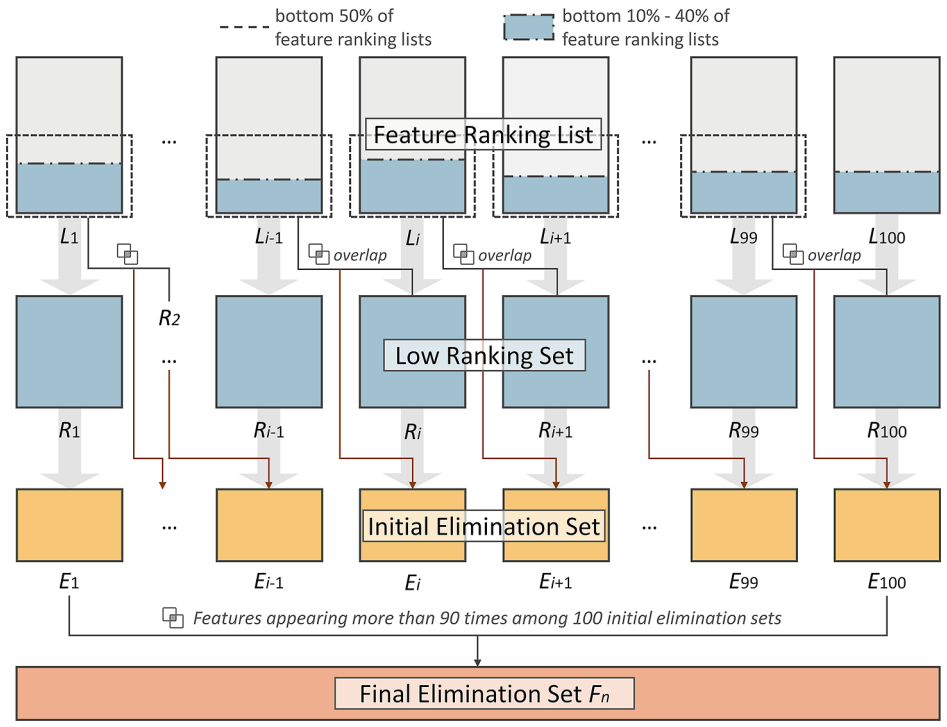

Figure 2. Schematic diagram of the novel FERCE algorithm. The FERCE algorithm conducts feature elimination based on ranking consensus evaluation. In sample group G_n, 100 feature ranking lists were generated by SVM-RFE, which were further processed by the FERCE algorithm. First, the features ranking in the bottom of the feature ranking list L_i (10 to 40% depending on the number of features in the feature ranking list) were put into a low-ranking set R_i. Second, for features in R_i, those ranking in the bottom 50% of L_{i-1} were put into an initial elimination set E_i to guarantee that they consistently ranked low among different feature ranking lists. The above two steps produced 100 different initial elimination sets. Third, features appearing more than 90 times among the 100 initial elimination sets were further put into the final elimination set F_n. All the k_n features in F_n were eliminated from the original feature set, and the remaining features formed the metabolomic signature of sample group G_n. A detailed description of each variable is provided in Table S1.

WHO Classification of Tumors.[33] Healthy volunteers (n = 175) with normal values on standard clinical tests of plasma and urine and without chronic medication or major illness were enrolled in the control group according to a physician's assessment. Nontargeted plasma metabolomic data from 288 subjects were acquired by liquid chromatography coupled to tandem mass spectrometry (LC−MS/MS). All details on sample preparation and data processing are provided in Supporting Information Methods.

Identification of a Robust Metabolomic Signature Using the Novel Strategy. The newly constructed robust identification strategy is a multivariate wrapper approach that integrates repeated random sampling and a consensus evaluation-based feature selection algorithm. It can minimize the error elimination of metabolic features, thus enabling the identification of robust metabolic features (RMFs).[34] The workflow of this strategy is illustrated in Figure 1. First, all 288 samples collected from the Xinqiao hospital were randomly divided into a discovery set and an independent test set. The discovery set contained 66 PA samples and 195 non-PA samples, and the independent test set contained 12 PA and 15 non-PA samples. Second, the discovery set was divided into a training set and a validation set by random sampling, where half of the samples were in the training set and the remaining samples were in the validation set. This random sampling process was repeated 2000 times, producing 2000 training-validation sets by pairing the training set with the validation set. The 2000 training-validation sets were then randomly divided into 20 groups, each containing 100 different training-validation sets. For each sample group, 100 training-validation sets were used to generate a metabolomic signature based on a consensus evaluation-based feature selection algorithm. This algorithm consists of two parts, namely, SVM-RFE[35] and feature elimination based on ranking consensus evaluation (FERCE), the latter of which is a novel algorithm proposed in this study. SVM-RFE has a successful application in the biomarker identification of metabolomic data, particularly in addressing challenges such as noisy training examples, a low number of biological replicates,[22] and nonlinearity among metabolites.[21]

Specifically, SVM-RFE built an SVM classifier based on the training set and evaluated the classification performance on the validation set. Meanwhile, the model assigned each feature a weight, which reflects the importance of the feature. According to the importance of features, the low-ranking features were removed, and the SVM was then retrained and evaluated using the remaining features. This process was repeated until the performance on the validation set began to degrade.[36] As a result, the SVM-RFE algorithm was used to generate 100 different feature ranking lists for 100 training-validation sets. Subsequently, in order to obtain a robust metabolomic signature from each group, these 100 feature ranking lists were further processed by the novel FERCE algorithm. The workflow of the FERCE algorithm is shown in Figure 2. For example, in sample group G_n, the procedure of the FERCE algorithm processing 100 feature ranking lists generated by SVM-RFE is as follows. (1) The features ranking in the bottom of the feature ranking list L_i (10 to 40% depending on the

https://doi.org/10.1021/acs.analchem.3c03796
Anal. Chem. XXXX, XXX, XXX−XXX

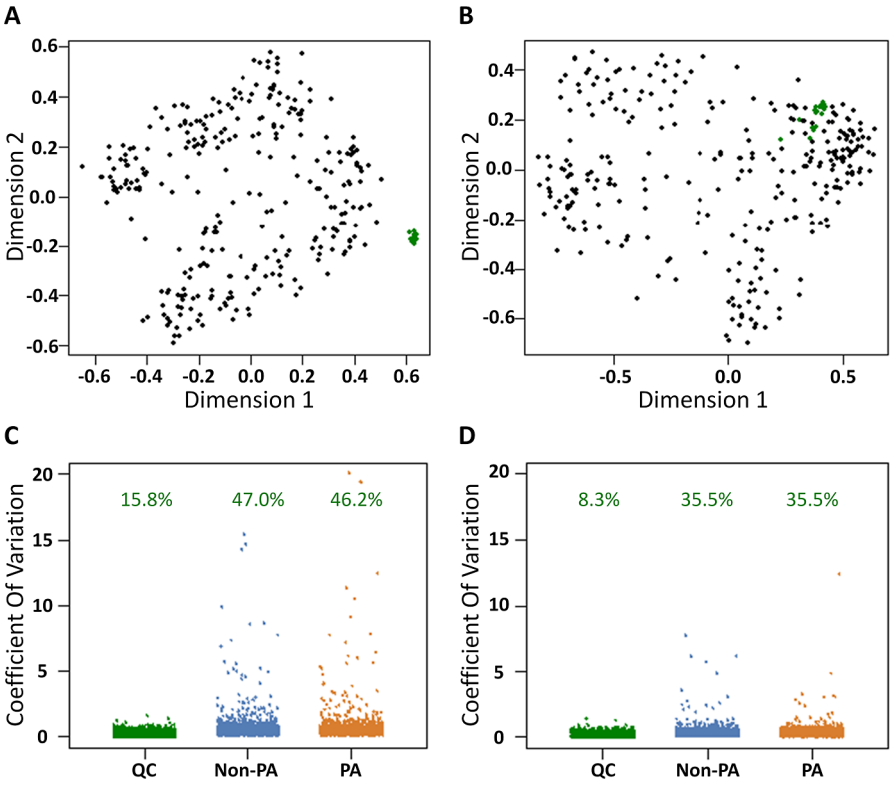

Figure 3. QC assessment on untargeted metabolomics data. (A) Visualization of samples in the ESI+ mode using an MDS plot. (B) Visualization of samples in the ESI− mode using an MDS plot. QC samples are shown as green dots. The PA and non-PA samples are shown as black dots. (C) Distribution of CVs in the ESI+ mode. (D) Distribution of CVs in the ESI− mode.

number of features in the feature ranking list) were put into a low-ranking set R_i. (2) For features in R_i, those ranking in the bottom 50% of L_{i-1} were put into an initial elimination set E_i to guarantee that they consistently ranked low among different feature ranking lists. The above two steps produced 100 different initial elimination sets. (3) Features that appeared more than 90 times among the 100 initial elimination sets were further put into the final elimination set F_n. (4) All the k_n features in F_n were eliminated from the original feature set, which contained m_n features, and the remaining $m_n - k_n$ features formed the metabolomic signature of sample group G_n. Finally, 20 metabolomic signatures containing varying numbers of differential metabolic features (DMFs) were identified. The intersection of 20 metabolomic signatures containing various RMFs was considered the robust metabolomic signature of PA and was selected as a potential metabolic biomarker for the diagnosis and treatment of PA. In this procedure, by removing these noisy features, we aim to retain informative features and minimize their impact on the model. Furthermore, eliminating these noisy features can also result in saving computational power.

Assessment on the Robustness of DMFs. In this study, a systematic assessment was performed to evaluate the robustness of the identified DMFs.[37] Metabolic data (discovery data) are first divided into 20 subdata sets using random sampling (20 times, half sample size for PA samples and half sample size for control samples, respectively). The random samples are then selected each time for PA samples and control samples and then combined for constructing 20 subdata sets. After the subgroup generation, the new approach for identifying the differential metabolic markers is applied to each subdata set. Based on the 20 marker sets identified from these 20 subdata sets, a powerful measure consistency score (CS)[37−39] is finally used to quantitatively evaluate the level of consistency among the 20 sets of identified metabolic markers. The higher CS represents more robust results in metabolic marker identification for that given data set. The CS is calculated using the selected differential metabolites in each subdata set based on the equation as follows

$$\mathrm{CS} = \sum_{i=2}^{C} \sum_{S \in I_i} 2^{i-2} \times n_S \tag{1}$$

where C indicates the total number of subdata sets and is equal to 20 in this study, I_i refers to a set of DMFs containing the intersections of any i subdata sets, and n_S represents the number of DMFs in the intersection S. In general, metabolic features selected by the approach are considered more robust when they yield more shared metabolic markers from more subdata sets, resulting in a higher CS.

Assessment on the Predictive Accuracy of Robust Metabolic Features. The predictive accuracy of selected features can reflect the effectiveness of the feature selection strategy.[40] In this study, the classification performance of RMFs identified from the discovery set was evaluated by using the SVM classification model to predict the PA outcomes on an independent test set.[41,42] The predictive performance was assessed using the accuracy metric (ACC),[43] which indicated the ratio of samples successfully predicted within the independent test set and was calculated by the following formula

$$\mathrm{ACC} = \frac{\mathrm{TP} + \mathrm{TN}}{\mathrm{TP} + \mathrm{FP} + \mathrm{TN} + \mathrm{FN}} \times 100\% \tag{2}$$

https://doi.org/10.1021/acs.analchem.3c03796
Anal. Chem. XXXX, XXX, XXX−XXX

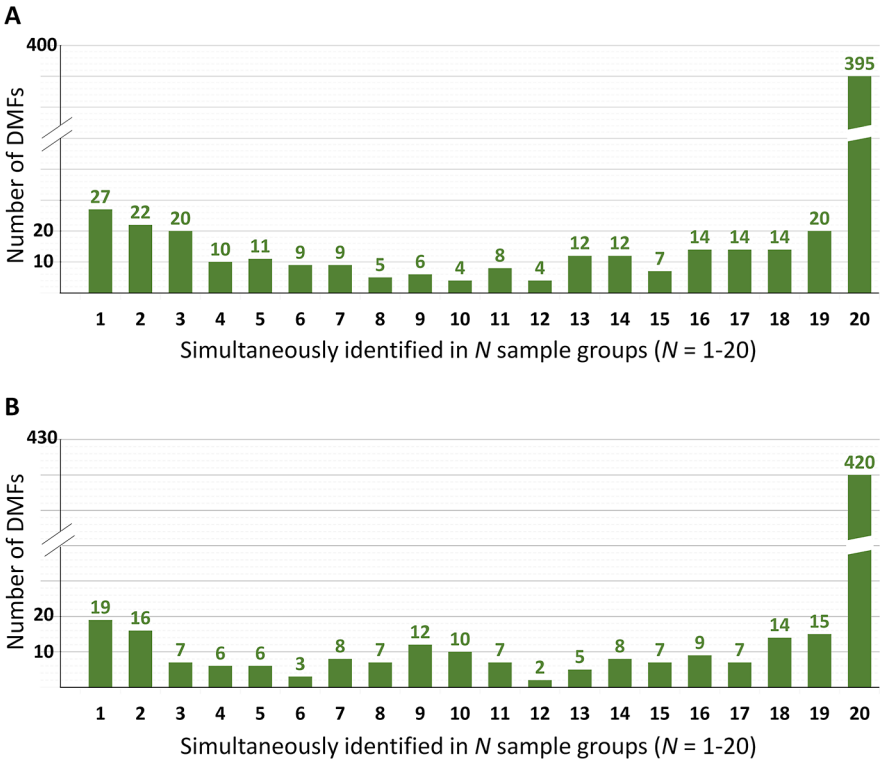

Figure 4. Number of DMFs identified simultaneously in N (N = 1−20) groups. (A) Number of DMFs identified simultaneously in N (N = 1−20) groups in the ESI+ mode. 395 DMFs were simultaneously discovered in all sample groups in the ESI+ mode, and only 27 DMFs were identified in a single sample group. (B) Number of DMFs identified simultaneously in N (N = 1−20) groups in the ESI− mode. 420 DMFs were simultaneously discovered in all sample groups in the ESI− mode, and only 19 DMFs were identified in a single sample group.

where TP, FP, TN, and FN represent the number of true positives, false positives, true negatives, and false negatives, respectively.

Biological Pathway Enrichment Analysis of RDMs. MSEA[44] on RDMs was conducted to identify biological pathways of significant enrichment.[45] In this study, Kyoto Encyclopedia of Genes and Genomes (KEGG)[44] and MetaboAnalyst 4.0[46] (https://www.metaboanalyst.ca/) were utilized to clarify relevant metabolic pathways. The list of RDMs identified by our novel strategy was used as input for MSEA. Various biological pathways along with their P-values were identified by MSEA. The Holm-Bonferroni method was applied to correct P-values, and the Holm-adjusted P-values were obtained.[47] Biological pathways with Holm-adjusted P-values less than 0.05 were defined as significantly enriched pathways and were considered to be closely associated with the development of PA.[48−50]

RESULTS AND DISCUSSION

QC Assessment of the Untargeted Metabolomics Data. The untargeted plasma metabolomics data acquisition was performed following the recommendations of the metabolomics quality assurance and quality control consortium (mQACC).[51] All the samples were divided into a discovery set and an independent test set. 261 participants, comprising 66 PA and 195 non-PA samples, constituted the discovery data set, and the independent test set was composed of 12 PA and 15 non-PA samples. The abundances of plasma small molecules (<1500 Da) in the discovery set and independent test set were measured by UPLC-ESI-QTOF/MS. After peak detection, alignment, peak area extraction, quality assurance, and missing values filtering,[52] a total of 3242 feature ions/signals were detected in the ESI+ mode and 1657 signals were detected in the ESI− mode. To handle missing values, we applied a method where the missing peaks were filled with half of the minimum peak area. The data, after the missing values were imputationed, were then used for subsequent differential metabolite analysis. The details on data preprocessing are demonstrated in Supporting Information Methods. These signals represented unique pairs of m/z and retention times; however, they did not correspond to specific metabolites. This is because the fragmentation process and adduct formation in MS can result in multiple signals representing a single metabolite. The overall workflow of this study is illustrated in Figure 1.

Quality control (QC) samples were also used to assess the quality and reproducibility of the measurement.[53,54] The multidimensional scaling (MDS) plot was applied to reduce the dimensionality of all samples and visualize the differences. The coefficients of variation (CVs) of features were utilized to assess the measurement variability based on QC samples. First, the MDS using Pearson's correlation coefficient as the distance metric was applied to reduce the dimensionality of all samples.[53] As shown in Figure 3A,B, black dots represented plasma samples, and green dots represented QC samples. In both modes, it was evident that QC samples were clustered together in the reduced-dimensional space, indicating QC variability is less than biological variability. Second, we assessed measurement variability using the CVs from QC samples. The CVs were calculated for all features, and the quality of measurement was quantitatively assessed by comparing the distributions of CVs between QC samples and plasma samples. As illustrated in Figure 3C,D, each point represented a specific

https://doi.org/10.1021/acs.analchem.3c03796
Anal. Chem. XXXX, XXX, XXX−XXX

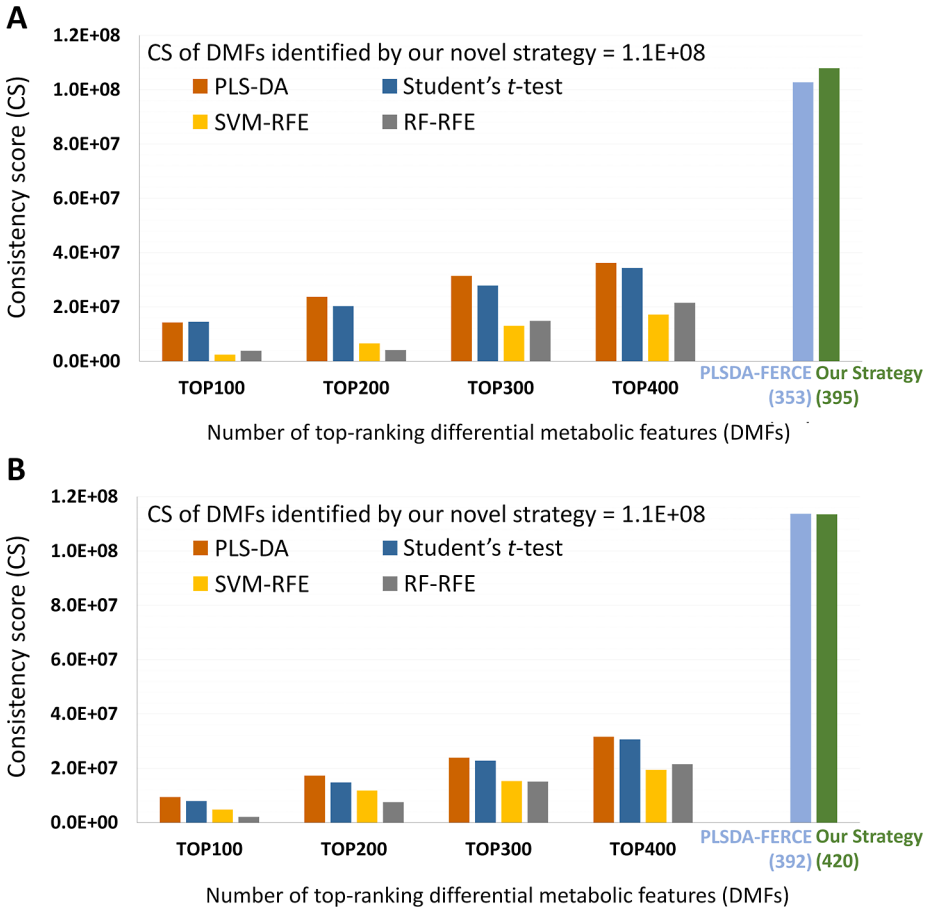

Figure 5. CS of the DMFs identified by PLS-DA, Student's *t*-test, SVM-RFE, RF-RFE, PLSDA-FERCE, and our proposed strategy. (A) CS of the DMFs identified by these methods in the ESI+ mode. (B) CS of the DMFs identified by these methods in the ESI− mode.

feature. The average CVs for all features within QC samples were 15.8 and 8.3% in the ESI+ mode and ESI− mode, respectively. These results demonstrated that most features showed acceptable repeatability with CVs <30% in QC samples.[55,56] It is noteworthy that the average CVs of QC samples were significantly lower than those of PA and non-PA (all *p*-values < 0.05) based on Student's *t*-test.[57] These observations indicate high measurement reproducibility.

Robustness of DMFs Identified by the Novel Strategy. First, we assess the algorithm's ability to select true positive metabolic features using the metabolomic data set MTBLS59.[58] This benchmark data set consists of the metabolic spectra of apple extracts detected by UPLC-MS (positive ionization mode) and contains 1632 metabolic features (22 true positive metabolic features). The data set includes 10 control samples and 3 spiked data sets of the same size, where spiked compounds were added in different concentrations. As demonstrated in Table S2, for each group, the algorithm identified 18, 15, and 14 true positive metabolic features out of the 22 spiking-in compounds, respectively. These results demonstrate the good performance of our approach in accurately selecting true positive metabolic features. In addition, to investigate the robustness of identified PA-associated DMFs, two commonly used metrics were employed in this study, as introduced in Materials and Methods. Specifically, 20 metabolomic signatures containing varying numbers of DMFs were generated from 20 sample groups based on the novel, robust identification strategy. As shown in Figure 4 and Tables S3 and S4, the number of DMFs identified from 20 sample groups varied from 501 to 508 in the ESI+ mode (Table S3) and from 501 to 510 in the ESI− mode (Table S4). There were 395 and 420 features simultaneously discovered in all sample groups in the ESI+ and ESI− modes, respectively, accounting for more than 77.8% (in the ESI+ mode) and 82.4% (in the ESI− mode) of identified DMFs. In addition, only 27 and 19 features were identified in a single sample group in the ESI+ and ESI− modes, respectively, accounting for less than 5.39% (in the ESI+ mode) and 3.79% (in the ESI− mode) of identified DMFs. These results indicated the high robustness of DMFs obtained from 20 sample groups.

Moreover, we provided a more comprehensive evaluation of the performance on robustness of the DMFs identified by our proposed approach. Particularly, we compared our newly proposed algorithm with five commonly used metabolic feature selection methods based on the CS of metabolite features identified for the discovery set. These methods included Student's *t*-test, PLS-DA, SVM-RFE, random forest recursive feature elimination (RF-RFE), and a consensus evaluation-based feature selection algorithm using PLS-DA (PLSDA-FERCE). Detailed descriptions of all five of these benchmark methods can be found in Supporting Information Methods. For the discovery set, the training and test sets were divided 1:1 using random seeds. The features were selected on the training set, and the selected features were evaluated on the CS. The comparison results for five metabolite feature

https://doi.org/10.1021/acs.analchem.3c03796
Anal. Chem. XXXX, XXX, XXX−XXX

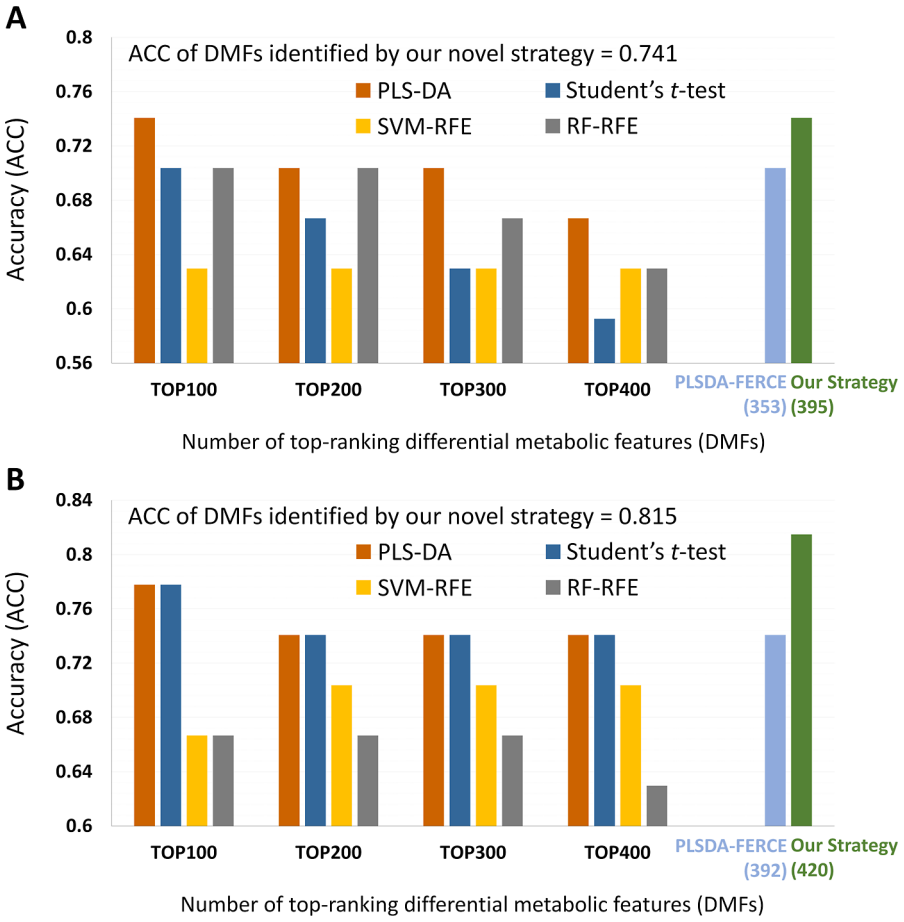

Figure 6. Predictive accuracy of the DMFs identified by PLS-DA, Student's *t*-test, SVM-RFE, RF-RFE, PLSDA-FERCE, and our proposed strategy. (A) Accuracy of the DMFs identified by these methods in the ESI+ mode. (B) Accuracy of the DMFs identified by these methods in the ESI− mode.

selection methods including Student's *t*-test, PLS-DA, SVM-RFE, RF-RFE, and PLSDA-FERCE are shown in Figure 5. As shown in Figure 5A, in the ESI+ mode, the CS of DMFs identified by benchmarked methods (Student's *t*-test, PLS-DA, SVM-RFE, and RF-RFE) increased with the enlargement of the number of selected top-ranking DMFs. Specifically, the CS of PLS-DA increased from 1.4×10^7 to 3.6×10^7 when the number of top-ranking DMFs increased from 100 to 400, the CS of Student's *t*-test increased from 1.5×10^7 to 3.4×10^7, the CS of SVM-RFE increased from 2.4×10^6 to 1.7×10^7, and the CS of RF-RFE increased from 3.9×10^6 to 2.2×10^7. Obviously, these CSs were substantially lower than that of our novel strategy, which was equal to 1.1×10^8. These results indicated a great enhancement in the robustness of the DMFs identified by our strategy. Similarly, Figure 5B illustrates that our novel strategy exhibited stronger robustness than that of Student's *t*-test, PLS-DA, SVM-RFE, and RF-RFE for the ESI− mode.

In current metabolomic studies, there are often nonlinear associations between metabolite concentrations and covariates, e.g., age, body mass index, gender, and hormone.[21] Additionally, there may exist nonlinear associations between PA phenotypes and covariates.[59,60] It is important to note that the RDMs discovered by the novel method may indeed be correlated or confounded by various factors such as diet or medication. These factors can significantly impact the interpretation and application of our findings. Therefore, further studies are necessary to determine the interplay between these metabolites and confounding factors.

Furthermore, we provided and released the source codes of the proposed novel algorithm. All the code for the proposed algorithm for selecting robust, discriminating metabolic features between distinct groups could be readily downloaded from the RMSI Web site (http:/rdblab.cn/rmsi/). The source code was freely accessible and could be utilized by users to analyze their own metabolomic data on local computers. The exemplar data input/output files could be simultaneously downloaded to assist users in understanding and applying the source code effectively. This is particularly beneficial for researchers or biologists without programming or mathematical backgrounds as it provides them with the necessary tools to screen robust, discriminating metabolic features.

Predictive Accuracy of Identified Robust Metabolic Features. The independent test set containing 27 plasma samples was employed to validate the predictive performance of the identified RMFs. The predictive ability of identified RMFs was evaluated on an independent test set using the SVM classification model. As a result, there was an overall improvement in the predictive ability of our novel strategy compared with that of other methods (Student's *t*-test, PLS-DA, SVM-RFE, RF-RFE, and PLSDA-FERCE). Specifically, as shown in Figure 6A (in the ESI+ mode), for TOP100, 200, 300, and 400 features, the ACC reached its highest values for Student's *t*-test, PLS-DA, SVM-RFE, and RF-RFE, with values

https://doi.org/10.1021/acs.analchem.3c03796
Anal. Chem. XXXX, XXX, XXX−XXX

of 0.704, 0.741, 0.630, and 0.704, respectively. PLSDA-FERCE achieved an ACC of 0.704. In contrast, the DMFs identified by our novel strategy achieved an ACC of 0.741. Similarly, as shown in Figure 6B (in the ESI− mode), the highest ACC values for Student's *t*-test, PLS-DA, SVM-RFE, and RF-RFE are 0.778, 0.778, 0.704, and 0.667, respectively. PLSDA-FERCE achieved an ACC of 0.741. In contrast, the ACC of DMFs identified by our novel strategy achieved a value of 0.815. These results indicated that the DMFs identified by the novel strategy exhibit better predictive accuracy in distinguishing PA from non-PA samples compared to those of other methods overall, especially for SVM-RFE and RF-RFE. Figure S1 demonstrates that the number of false positives (FP) obtained by our novel strategy is generally lower than that of other methods when they are applied to predict independent test data.

Moreover, we also compared the predictive ability of the robust metabolic features identified by the proposed method using five machine learning classifiers based on independent test data. These five machine learning classifiers, widely utilized in the metabolomics field, include SVM,[61] RF,[62] XGBoost,[63] naive Bayes (NB),[64] and K-nearest neighbor (kNN).[65] The classifiers were trained using the 395 robust metabolic features selected in the positive mode and the 420 robust metabolic features selected in the negative mode for the discovery data set. The performance of the classifier models was then evaluated on the basis of the independent test data. The performance comparison results for these five classifiers are listed in Table 1. As shown in Table 1, when applied to the independent set, the SVM classifier yielded accuracy values of 0.74 (for POS) and 0.81 (for NEG). These results demonstrate a good predictive capability, outperforming other classifiers such as RF, XGBoost, NB, and kNN.

Table 1. Performance Comparison of Five Machine Learning Classifiers Using the Robust Metabolic Features Selected by the Proposed Approach in This Study[a]

method	abbreviation	accuracy (ACC)	false negatives (FN)	false positives (FP)
support vector machine	SVM	NEG (0.81)	NEG (2)	NEG (3)
		POS (0.74)	POS (2)	POS (5)
random forest	RF	NEG (0.74)	NEG (2)	NEG (5)
		POS (0.67)	POS (1)	POS (8)
XGBoost	XGB	NEG (0.78)	NEG (2)	NEG (4)
		POS (0.56)	POS (8)	POS (4)
naive Bayes	NB	NEG (0.74)	NEG (0)	NEG (7)
		POS (0.67)	POS (1)	POS (8)
K-nearest neighbor	kNN	NEG (0.63)	NEG (7)	NEG (3)
		POS (0.56)	POS (3)	POS (9)

[a]395 features were screened from metabolomic data in the positive ion mode and 420 features in the negative ion mode. The classifiers were trained on the discovery data and applied to predict the independent test set.

Biological Relevance of PA-Specific RDMs. The newly constructed strategy was developed to identify PA-specific RDMs. All the RDMs were annotated based on the commercial databases *MetDDA* and *LipDDA* (Supporting Information Methods). As shown in Table S5, a robust signature containing 45 RDMs was identified. In sum, these 45 significantly differential plasma metabolites included different kinds of amino acids, steroids, sphingolipids, bile acids, nucleotides, fatty acids, lipoglycans, and hydroxy acids. As reported previously, bile acids (such as lithocholic acid and cholic acid) promoted the production of reactive oxygen species and thus caused DNA damage in cancer.[66] Moreover, some RDMs discovered in this study played key roles in the development of PA. Specifically, 18 metabolites have been reported to be associated with the pathogenesis of PA in previous studies, including hydrocortisone,[67] arachidonic acid,[68] L-citrulline,[69] inosine,[70,71] L-arginine,[72] lipopolysaccharide (LPS)[73] (including LPS (18:0/0:0), LPS (18:2/0:0), LPS (20:0/0:0), LPS (20:4/0:0), LPS (22:2/0:0), LPS (22:6/0:0), and LPS (24:4/0:0)), *trans*-vaccenic acid,[74] beta-hydroxybutyrate,[75] L-glutamate,[76] caprylic acid,[10,77] phosphatidylcholine (PC) (17:1/22:6),[76,78] and phosphatidylethanolamine (PE) (18:1/0:0).[10] Considering arachidonic acid, for example, previous studies have investigated the involvement of arachidonic acid metabolites in basal and thyrotropin-releasing hormone-stimulated prolactin release in GH3 cells, a cloned strain of rat pituitary tumor cells.[68] It has also been reported that arachidonic acid plays a vital role in the regulation of adrenocorticotropin release.[68] In addition, arachidonic acid can induce the activation of PPAR-γ,[79] which is highly expressed in pituitary tumors and is an important molecular target of PA.[80] The biological relevance between these identified robust metabolites and PA was comprehensively reviewed and is provided in Supporting Information Methods.

Robust Metabolomic Signature Reflects the Altered Lipid Metabolism in PA. MSEA is a valuable approach for determining the biological functions associated with the identified differential metabolites. By conducting a secondary analysis, MSEA enables the collective exploration of these metabolites and enhances our understanding of their underlying biological mechanisms. Exploring dysregulated biological pathways in PA is essential for comprehending the pathology of PA. Thus, MSEA was performed to investigate the biological pathways associated with the 45 identified RDMs. Based on KEGG pathway mapping, as demonstrated in Table S5, the majority of the identified metabolites were involved in lipid metabolism, amino acid metabolism, glycan biosynthesis and metabolism, and nucleotide metabolism. Among these biological pathways, some have been reported to be closely related to the pathogenesis of PA. For instance, the progression of PA is associated with alterations in amino acid metabolism.[14] In addition, the glycan biosynthesis and metabolism pathway was found to play a vital role in the development of PA based on transcriptomic analysis.[81] Moreover, the activation of nucleotide metabolism has been confirmed as a response to thyroid hormone-stimulated cell proliferation, providing valuable insights into the molecular mechanisms underlying PA pathogenesis.[82]

In this study, MSEA further revealed the altered lipid metabolism in PA. The results of MSEA are displayed in Table 2. A total of 12 pathways were identified as enriched, with primary bile acid biosynthesis exhibiting the most significant enrichment among them (Holm-adjusted *P*-value = 0.0047).

https://doi.org/10.1021/acs.analchem.3c03796
Anal. Chem. XXXX, XXX, XXX−XXX

Table 2. Results of Metabolite Set Enrichment Analysis Based on the 45 Robust Differential Metabolites[a]

pathway name	pathway classification	total	expected	hits	raw *P*-value	−log(*P*)	Holm-adjusted *P*-value
primary bile acid biosynthesis	lipid metabolism	47	0.45	5	5.91×10^{-5}	9.736	0.005
arginine and proline metabolism	amino acid metabolism	77	0.74	4	0.005	5.222	0.427
aminoacyl-tRNA biosynthesis	translation	75	0.72	3	0.033	3.412	1
D-arginine and D-ornithine metabolism	metabolism of other amino acids	8	0.08	1	0.074	2.603	1
fatty acid biosynthesis	lipid metabolism	49	0.47	2	0.078	2.547	1
D-glutamate metabolism	metabolism of other amino acids	11	0.11	1	0.100	2.298	1
tryptophan metabolism	amino acid metabolism	79	0.75	2	0.173	1.754	1
caffeine metabolism	biosynthesis of secondary metabolites	21	0.20	1	0.183	1.697	1
alanine, aspartate, and glutamate metabolism	amino acid metabolism	24	0.23	1	0.207	1.577	1
sphingolipid metabolism	lipid metabolism	25	0.24	1	0.214	1.540	1
purine metabolism	nucleotide metabolism	92	0.88	2	0.219	1.520	1
fatty acid elongation in mitochondria	lipid metabolism	27	0.26	1	0.230	1.472	1

[a]All the pathways are sorted in ascending order of the raw *P*-value.

There were five hits in primary bile acid biosynthesis among the 45 identified RDMs, namely, chenodeoxycholic acid glycine conjugate, taurochenodesoxycholic acid, glycocholic acid, chenodeoxycholic acid, and cholic acid, as illustrated in Figure S2. All these five metabolites were categorized as bile acids and were involved in lipid metabolism, reflecting the alteration of lipid metabolism in PA. Lipids serve various crucial functions, including their involvement in cell membrane formation, energy provision, and cell signaling transduction. Other omics studies, such as proteomic signaling pathway network analysis, have revealed the underlying alterations in lipid metabolism associated with PA, which are consistent with the findings of our study.[83] Our findings provided new insights into robust metabolic biomarkers for the diagnosis and treatment of PA.

CONCLUSIONS

In this study, we performed global untargeted plasma metabolomic profiling and identified a robust PA-specific metabolomic signature using a novel robust identification strategy. This novel strategy integrates repeated random sampling and a consensus evaluation-based feature selection algorithm and can evaluate the consistency of metabolomic signatures obtained from different sample groups. A systematic assessment of this novel strategy demonstrated its enhanced robustness and better discriminative performance compared to that of other feature selection methods including Student's *t*-test, PLS-DA, SVM-RFE, and RF-RFE. The identified robust metabolomic signature comprised 45 metabolites discriminating PA from non-PA. Moreover, the MSEA of these metabolites reflected the alterations in lipid metabolism in PA. These findings can facilitate an in-depth understanding of the molecular mechanisms underlying the pathogenesis of PA and provide important insights for discovering diagnostic molecules and potential drug targets for PA. We believe the proposed strategy stands as a valuable tool for screening robust, discriminating metabolic features within the field of metabolomics.

ASSOCIATED CONTENT

Supporting Information

The Supporting Information is available free of charge at https://pubs.acs.org/doi/10.1021/acs.analchem.3c03796.

Methods for sample preparation and untargeted metabolic profiling, QC and data processing, introduction of metabolic feature selection methods, biological relevance of identified RDMs, description of each variable in the workflow of the newly constructed strategy, results of the robust metabolic features selected using the proposed approach on spiked-in metabolomic data, statistics of DMFs identified from 20 sample groups in the ESI+ and ESI− modes and 45 identified PA-specific RDMs, number of FNs and FPs obtained by our novel strategy and five other methods, and map of the primary bile acid biosynthesis pathway (PDF)

AUTHOR INFORMATION

Corresponding Authors

Feng Zhu − *College of Pharmaceutical Sciences, The Second Affiliated Hospital, Zhejiang University School of Medicine, Zhejiang University, Hangzhou 310058, China; Innovation Institute for Artificial Intelligence in Medicine of Zhejiang University, Alibaba-Zhejiang University Joint Research Center of Future Digital Healthcare, Hangzhou 330110, China*; orcid.org/0000-0001-8069-0053; Email: zhufeng@zju.edu.cn

Hui Yang − *Multidisciplinary Center for Pituitary Adenoma of Chongqing, Department of Neuosurgery, Xinqiao Hospital, Army Medical University, Chongqing 400037, China*; Email: huiyangxinqiao@163.com

Song Li − *Multidisciplinary Center for Pituitary Adenoma of Chongqing, Department of Neuosurgery, Xinqiao Hospital, Army Medical University, Chongqing 400037, China*; Email: dlisong3@163.com

Authors

Jing Tang − *College of Pharmaceutical Sciences, The Second Affiliated Hospital, Zhejiang University School of Medicine, Zhejiang University, Hangzhou 310058, China; Department of Bioinformatics, Chongqing Medical University, Chongqing 400016, China*

Minjie Mou − *College of Pharmaceutical Sciences, The Second Affiliated Hospital, Zhejiang University School of Medicine, Zhejiang University, Hangzhou 310058, China*; orcid.org/0000-0001-7619-2975

Xin Zheng − *Multidisciplinary Center for Pituitary Adenoma of Chongqing, Department of Neuosurgery, Xinqiao Hospital, Army Medical University, Chongqing 400037, China*

https://doi.org/10.1021/acs.analchem.3c03796
Anal. Chem. XXXX, XXX, XXX−XXX

Jin Yan − *Multidisciplinary Center for Pituitary Adenoma of Chongqing, Department of Neuosurgery, Xinqiao Hospital, Army Medical University, Chongqing 400037, China*
Ziqi Pan − *College of Pharmaceutical Sciences, The Second Affiliated Hospital, Zhejiang University School of Medicine, Zhejiang University, Hangzhou 310058, China;* orcid.org/0000-0002-3883-4161
Jinsong Zhang − *College of Pharmaceutical Sciences, The Second Affiliated Hospital, Zhejiang University School of Medicine, Zhejiang University, Hangzhou 310058, China*
Bo Li − *School of Pharmaceutical Sciences, Chongqing University, Chongqing 401331, China*
Qingxia Yang − *School of Pharmaceutical Sciences, Chongqing University, Chongqing 401331, China;* orcid.org/0000-0001-9607-7026
Yunxia Wang − *College of Pharmaceutical Sciences, The Second Affiliated Hospital, Zhejiang University School of Medicine, Zhejiang University, Hangzhou 310058, China;* orcid.org/0000-0003-1951-942X
Ying Zhang − *College of Pharmaceutical Sciences, The Second Affiliated Hospital, Zhejiang University School of Medicine, Zhejiang University, Hangzhou 310058, China*
Jianqing Gao − *College of Pharmaceutical Sciences, The Second Affiliated Hospital, Zhejiang University School of Medicine, Zhejiang University, Hangzhou 310058, China;* orcid.org/0000-0003-1052-7060

Complete contact information is available at: https://pubs.acs.org/10.1021/acs.analchem.3c03796

Author Contributions

#J.T., M.M., and X.Z. contributed equally to this work as cofirst authors.

Notes

The authors declare no competing financial interest.

■ ACKNOWLEDGMENTS

This work was supported by the National Natural Science Foundation of China [82373790, 82301909, 22220102001, U1909208, 81872798, and 81971982]; the Natural Science Foundation of Zhejiang Province [LR21H300001]; the National Key R&D Program of China [2022YFC3400501]; the Leading Talent of the "Ten Thousand Plan" National High-Level Talents Special Support Plan of China; the Double Top-Class Universities [181201*194232101]; the Fundamental Research Funds for Central Universities [2018QNA7023]; the Key R&D Program of Zhejiang Province [2020C03010]; Westlake Laboratory (Westlake Laboratory of Life Science & Biomedicine); the Alibaba-Zhejiang University Joint Research Center of Future Digital Healthcare; Alibaba Cloud; and the Information Technology Center of Zhejiang University. Funding for open access charge: the Natural Science Foundation of Zhejiang Province [LR21H300001].

■ REFERENCES

(1) Salomon, M. P.; Wang, X.; Marzese, D. M.; Hsu, S. C.; Nelson, N.; Zhang, X.; Matsuba, C.; Takasumi, Y.; Ballesteros-Merino, C.; Fox, B. A.; Barkhoudarian, G.; Kelly, D. F.; Hoon, D. S. B. *Clin. Cancer Res.* **2018**, *24*, 4126−4136.
(2) Nota, N. M.; Wiepjes, C. M.; de Blok, C. J. M.; Gooren, L. J. G.; Peerdeman, S. M.; Kreukels, B. P. C.; den Heijer, M. *Brain* **2018**, *141*, 2047−2054.
(3) Aste, L.; Bellinzona, M.; Meleddu, V.; Farci, G.; Manieli, C.; Godano, U. *J. Oncol.* **2010**, *2010*, 195323.
(4) Inoshita, N.; Nishioka, H. *Brain Tumor Pathol.* **2018**, *35*, 51−56.
(5) Lecoq, A. L.; Kamenicky, P.; Guiochon-Mantel, A.; Chanson, P. *Nat. Rev. Endocrinol.* **2015**, *11*, 43−54.
(6) Zhu, H.; Guo, J.; Shen, Y.; Dong, W.; Gao, H.; Miao, Y.; Li, C.; Zhang, Y. *Clin. Cancer Res.* **2018**, *24*, 5757−5766.
(7) Mehta, G. U.; Lonser, R. R. *Neuro Oncol.* **2017**, *19*, 762−773.
(8) Pozza, C.; Graziadio, C.; Giannetta, E.; Lenzi, A.; Isidori, A. M. *J. Oncol.* **2012**, *2012*, 685213.
(9) Beckers, A.; Aaltonen, L. A.; Daly, A. F.; Karhu, A. *Endocr. Rev.* **2013**, *34*, 239−277.
(10) Pinzariu, O.; Georgescu, B.; Georgescu, C. E. *Front. Endocrinol.* **2019**, *9*, 814.
(11) Zheng, X.; Li, S.; Zhang, W. H.; Yang, H. *Diabetes Metab. Syndr. Obes.* **2015**, *8*, 357−361.
(12) Auriemma, R. S.; De Alcubierre, D.; Pirchio, R.; Pivonello, R.; Colao, A. *Front. Endocrinol.* **2019**, *10*, 327.
(13) Molitch, M. E. *JAMA, J. Am. Med. Assoc.* **2017**, *317*, 516−524.
(14) Oklu, R.; Deipolyi, A. R.; Wicky, S.; Ergul, E.; Deik, A. A.; Chen, J. W.; Hirsch, J. A.; Wojtkiewicz, G. R.; Clish, C. B. *J. Neurointerv. Surg.* **2014**, *6*, 541−546.
(15) Zhan, X.; Desiderio, D. M. *Mass Spectrom. Rev.* **2005**, *24*, 783−813.
(16) Onguru, O.; Scheithauer, B. W.; Kovacs, K.; Vidal, S.; Jin, L.; Zhang, S.; Ruebel, K. H.; Lloyd, R. V. *Mod. Pathol.* **2004**, *17*, 772−780.
(17) Ijare, O.; Baskin, D. S.; Pichumani, K. *Neuro Oncol.* **2017**, *19*, 145.
(18) Lin, K.; Zhang, J.; Lin, Y.; Pei, Z.; Wang, S. *Front. Endocrinol.* **2022**, *13*, 901884.
(19) Banerjee, A.; Halder, A.; Jadhav, P.; Bankar, R.; Pattarkine, J.; Hole, A.; Shah, A.; Goel, A.; Murali Krishna, C.; Srivastava, S. *Anal. Chem.* **2022**, *94*, 11898−11907.
(20) Rizzo, R.; Lisboa, P. J. *BMC Bioinf.* **2013**, *14* (S1), I1.
(21) Takahashi, Y.; Ueki, M.; Yamada, M.; Tamiya, G.; Motoike, I. N.; Saigusa, D.; Sakurai, M.; Nagami, F.; Ogishima, S.; Koshiba, S.; Kinoshita, K.; Yamamoto, M.; Tomita, H. *Transl. Psychiatry* **2020**, *10*, 157.
(22) Heinemann, J.; Mazurie, A.; Tokmina-Lukaszewska, M.; Beilman, G. J.; Bothner, B. *Metabolomics* **2014**, *10*, 1121−1128.
(23) Dreyfuss, J. M.; Johnson, M. D.; Park, P. J. *Mol. Cancer* **2009**, *8*, 71.
(24) Armitage, E. G.; Barbas, C. *J. Pharm. Biomed. Anal.* **2014**, *87*, 1−11.
(25) Xia, J.; Broadhurst, D. I.; Wilson, M.; Wishart, D. S. *Metabolomics* **2013**, *9*, 280−299.
(26) Li, F.; Yin, J.; Lu, M.; Yang, Q.; Zeng, Z.; Zhang, B.; Li, Z.; Qiu, Y.; Dai, H.; Chen, Y.; Zhu, F. *Brief. Bioinformatics* **2022**, *23*, bbac253.
(27) Fu, J.; Zhang, Y.; Wang, Y.; Zhang, H.; Liu, J.; Tang, J.; Yang, Q.; Sun, H.; Qiu, W.; Ma, Y.; Li, Z.; Zheng, M.; Zhu, F. *Nat. Protoc.* **2022**, *17*, 129−151.
(28) Christin, C.; Hoefsloot, H. C.; Smilde, A. K.; Hoekman, B.; Suits, F.; Bischoff, R.; Horvatovich, P. *Mol. Cell. Proteomics* **2013**, *12*, 263−276.
(29) Yang, Q.; Wang, Y.; Zhang, Y.; Li, F.; Xia, W.; Zhou, Y.; Qiu, Y.; Li, H.; Zhu, F. *Nucleic Acids Res.* **2020**, *48*, W436−W448.
(30) Kim, S. Y. *BMC Bioinf.* **2009**, *10*, 147.
(31) Jaakkola, M. K.; Seyednasrollah, F.; Mehmood, A.; Elo, L. L. *Brief. Bioinformatics* **2017**, *18*, 735−743.
(32) Wang, L.; Gong, Y.; Chippada-Venkata, U.; Heck, M. M.; Retz, M.; Nawroth, R.; Galsky, M.; Tsao, C. K.; Schadt, E.; de Bono, J.; Olmos, D.; Zhu, J.; Oh, W. K. *BMC Med.* **2015**, *13*, 201.
(33) Grossman, A. B. *Acta Neuropathol.* **2006**, *111*, 76−77.
(34) Yang, Q.; Li, B.; Tang, J.; Cui, X.; Wang, Y.; Li, X.; Hu, J.; Chen, Y.; Xue, W.; Lou, Y.; Qiu, Y.; Zhu, F. *Brief. Bioinformatics* **2020**, *21*, 1058−1068.
(35) Yang, Q.; Gong, Y.; Zhu, F. *Anal. Chem.* **2023**, *95*, 5542−5552.
(36) Yang, Q.; Li, B.; Wang, P.; Xie, J.; Feng, Y.; Liu, Z.; Zhu, F. *Brief. Bioinformatics* **2022**, *23*, bbac455.

(37) Tang, J.; Fu, J.; Wang, Y.; Li, B.; Li, Y.; Yang, Q.; Cui, X.; Hong, J.; Li, X.; Chen, Y.; Xue, W.; Zhu, F. *Brief. Bioinformatics* **2020**, *21*, 621−636.
(38) Yang, Q.; Li, B.; Chen, S.; Tang, J.; Li, Y.; Li, Y.; Zhang, S.; Shi, C.; Zhang, Y.; Mou, M.; Xue, W.; Zhu, F. *J. Proteomics* **2021**, *232*, 104023.
(39) Wang, X.; Gardiner, E. J.; Cairns, M. J. *Mol. Biosyst.* **2015**, *11*, 1235−1240.
(40) Wu, Y.; Yang, L.; Wu, X.; Wang, L.; Qi, H.; Feng, Q.; Peng, B.; Ding, Y.; Tang, J. *FASEB J.* **2023**, *37*, No. e23056.
(41) Di Poto, C.; Ferrarini, A.; Zhao, Y.; Varghese, R. S.; Tu, C.; Zuo, Y.; Wang, M.; Nezami Ranjbar, M. R.; Luo, Y.; Zhang, C.; Desai, C. S.; Shetty, K.; Tadesse, M. G.; Ressom, H. W. *Cancer Epidemiol. Biomarkers Prev.* **2017**, *26*, 675−683.
(42) Min, S.; Lee, B.; Yoon, S. *Brief. Bioinformatics* **2017**, *18*, 851−869.
(43) Song, L.; Zhuang, P.; Lin, M.; Kang, M.; Liu, H.; Zhang, Y.; Yang, Z.; Chen, Y.; Zhang, Y. *J. Proteome Res.* **2017**, *16*, 3180−3189.
(44) Xia, J.; Wishart, D. *Nucleic Acids Res.* **2010**, *38*, W71−W77.
(45) Merino, J.; Leong, A.; Liu, C. T.; Porneala, B.; Walford, G. A.; von Grotthuss, M.; Wang, T. J.; Flannick, J.; Dupuis, J.; Levy, D.; Gerszten, R. E.; Florez, J. C.; Meigs, J. B. *Diabetologia* **2018**, *61*, 1315−1324.
(46) Chong, J.; Soufan, O.; Li, C.; Caraus, I.; Li, S.; Bourque, G.; Wishart, D. S.; Xia, J. *Nucleic Acids Res.* **2018**, *46*, W486−W494.
(47) Perry, B. I.; Burgess, S.; Jones, H. J.; Zammit, S.; Upthegrove, R.; Mason, A. M.; Day, F. R.; Langenberg, C.; Wareham, N. J.; Jones, P. B.; Khandaker, G. *PLoS Med.* **2021**, *18*, No. e1003455.
(48) Kalla, R.; Adams, A. T.; Bergemalm, D.; Vatn, S.; Kennedy, N. A.; Ricanek, P.; Lindstrom, J.; Ocklind, A.; Hjelm, F.; Ventham, N. T.; Ho, G. T.; Petren, C.; Repsilber, D.; Soderholm, J.; Pierik, M.; D'Amato, M.; Gomollon, F.; Olbjorn, C.; Jahnsen, J.; Vatn, M. H.; Halfvarson, J.; Satsangi, J. *J. Crohns Colitis* **2021**, *15*, 699−708.
(49) Gupta, S.; Vundavilli, H.; Osorio, R. S. A.; Itoh, M. N.; Mohsen, A.; Datta, A.; Mizuguchi, K.; Tripathi, L. P. *IEEE J. Biomed. Health Inform.* **2022**, *26*, 4785−4793.
(50) Kourou, K.; Papaloukas, C.; Fotiadis, D. I. *IEEE J. Biomed. Health Inform.* **2017**, *21*, 320−327.
(51) Kirwan, J. A.; Gika, H.; Beger, R. D.; Bearden, D.; Dunn, W. B.; Goodacre, R.; Theodoridis, G.; Witting, M.; Yu, L. R.; Wilson, I. D.; metabolomics Quality, A.; Quality Control, C. *Metabolomics* **2022**, *18*, 70.
(52) Dunn, W.; Broadhurst, D.; Begley, P.; Zelena, E.; Francis-McIntyre, S.; Anderson, N.; Brown, M.; Knowles, J. D.; Halsall, A.; Haselden, J. N.; Nicholls, A. W.; Wilson, I. D.; Kell, D. B.; Goodacre, R. *Nat. Protoc.* **2011**, *6*, 1060−1083.
(53) Becavin, C.; Tchitchek, N.; Mintsa-Eya, C.; Lesne, A.; Benecke, A. *Bioinformatics* **2011**, *27*, 1413−1421.
(54) Blanco-Almazan, D.; Groenendaal, W.; Lijnen, L.; Onder, R.; Smeets, C.; Ruttens, D.; Catthoor, F.; Jane, R. *IEEE J. Biomed. Health Inform.* **2022**, *26*, 5983−5991.
(55) Xu, H.; Xu, Y.; Zhao, G.; Fu, X.; Zhao, J.; Wang, H.; Cai, Y.; Lin, H. *Mol. Omics* **2023**, *19*, 418−428.
(56) Saberi Hosnijeh, F.; Pechlivanis, A.; Keun, H. C.; Portengen, L.; Bueno-de-Mesquita, H. B.; Heederik, D.; Vermeulen, R. *Environ. Mol. Mutagen.* **2013**, *54*, 558−565.
(57) Tworoger, S. S.; Spentzos, D.; Grall, F. T.; Liebermann, T. A.; Hankinson, S. E. *Cancer Epidemiol. Biomarkers Prev.* **2008**, *17*, 1480−1485.
(58) Franceschi, P.; Masuero, D.; Vrhovsek, U.; Mattivi, F.; Wehrens, R. *J. Chemom.* **2012**, *26*, 16−24.
(59) Seki, Y.; Ichihara, A. *PLoS One* **2022**, *17*, No. e0267324.
(60) Galm, B. P.; Martinez-Salazar, E. L.; Swearingen, B.; Torriani, M.; Klibanski, A.; Bredella, M. A.; Tritos, N. A. *Eur. J. Endocrinol.* **2018**, *179*, 191−198.
(61) de Boves Harrington, P. *Anal. Chem.* **2015**, *87*, 11065−11071.
(62) Chen, N.; Wang, H. B.; Wu, B. Q.; Jiang, J. H.; Yang, J. T.; Tang, L. J.; He, H. Q.; Linghu, D. D. *Talanta* **2021**, *235*, 122720.
(63) Zhang, Y.; Sylvester, K. G.; Jin, B.; Wong, R. J.; Schilling, J.; Chou, C. J.; Han, Z.; Luo, R. Y.; Tian, L.; Ladella, S.; Mo, L.; Maric, I.; Blumenfeld, Y. J.; Darmstadt, G. L.; Shaw, G. M.; Stevenson, D. K.; Whitin, J. C.; Cohen, H. J.; McElhinney, D. B.; Ling, X. B. *Metabolites* **2023**, *13*, 715.
(64) Adam, M. G.; Beyer, G.; Christiansen, N.; Kamlage, B.; Pilarsky, C.; Distler, M.; Fahlbusch, T.; Chromik, A.; Klein, F.; Bahra, M.; Uhl, W.; Grutzmann, R.; Mahajan, U. M.; Weiss, F. U.; Mayerle, J.; Lerch, M. M. *Gut* **2021**, *70*, 2150−2158.
(65) Wang, H.; Wang, Y.; Li, X.; Deng, X.; Kong, Y.; Wang, W.; Zhou, Y. *Cardiovasc. Diabetol.* **2022**, *21*, 288.
(66) Hanahan, D.; Weinberg, R. A. *Cell* **2011**, *144*, 646−674.
(67) Bonzo, J. A.; Patterson, A. D.; Krausz, K. W.; Gonzalez, F. J. *Mol. Endocrinol.* **2010**, *24*, 2343−2355.
(68) Rabier, M.; Chavis, C.; de Paulet, A.; Damon, M. *Prostaglandins Leukot. Med.* **1987**, *27*, 27−42.
(69) Lloyd, R. V.; Jin, L.; Qian, X.; Zhang, S.; Scheithauer, B. W. *Am. J. Pathol.* **1995**, *146*, 86−94.
(70) Anand-Srivastava, M. B.; Cantin, M.; Gutkowska, J. *Mol. Cell. Biochem.* **1989**, *89*, 21−28.
(71) Zinshteyn, B.; Nishikura, K. *Wiley Interdiscip Rev. Syst. Biol. Med.* **2009**, *1*, 202−209.
(72) Martino, E. *J. Endocrinol. Invest.* **1999**, *22*, 89.
(73) De Laurentiis, A.; Pisera, D.; Caruso, C.; Candolfi, M.; Mohn, C.; Rettori, V.; Seilicovich, A. *Neuroimmunomodulation* **2002**, *10*, 30−39.
(74) Da Silva, M. S.; Julien, P.; Perusse, L.; Vohl, M. C.; Rudkowska, I. *Lipids* **2015**, *50*, 873−882.
(75) Laeger, T.; Metges, C. C.; Kuhla, B. *Appetite* **2010**, *54*, 450−455.
(76) Caruso, C.; Bottino, M. C.; Pampillo, M.; Pisera, D.; Jaita, G.; Duvilanski, B.; Seilicovich, A.; Lasaga, M. *Endocrinology* **2004**, *145*, 4677−4684.
(77) Feng, J.; Zhang, Q.; Zhou, Y.; Yu, S.; Hong, L.; Zhao, S.; Yang, J.; Wan, H.; Xu, G.; Zhang, Y.; Li, C. *Front. Endocrinol.* **2018**, *9*, 678.
(78) Einstien, A.; Virani, R. *J. Clin. Diagn. Res.* **2016**, *10*, TC01−04.
(79) Dozsa, A.; Dezso, B.; Toth, B. I.; Bacsi, A.; Poliska, S.; Camera, E.; Picardo, M.; Zouboulis, C. C.; Biro, T.; Schmitz, G.; Liebisch, G.; Ruhl, R.; Remenyik, E.; Nagy, L. *J. Invest. Dermatol.* **2014**, *134*, 910−920.
(80) Heaney, A. P.; Fernando, M.; Melmed, S. *J. Clin. Invest.* **2003**, *111*, 1381−1388.
(81) Zhao, P.; Hu, W.; Wang, H.; Yu, S.; Li, C.; Bai, J.; Gui, S.; Zhang, Y. *Int. J. Endocrinol.* **2015**, *2015*, 164087.
(82) Miller, L. D.; Park, K. S.; Guo, Q. M.; Alkharouf, N. W.; Malek, R. L.; Lee, N. H.; Liu, E. T.; Cheng, S. Y. *Mol. Cell. Biol.* **2001**, *21*, 6626−6639.
(83) Zhan, X.; Desiderio, D. M. *BMC Med. Genom.* **2010**, *3*, 13.

https://doi.org/10.1021/acs.analchem.3c03796
Anal. Chem. XXXX, XXX, XXX−XXX